

9-30-2015

Ion Bombardment of Ni(110) Studied with Inverse Photoemission Spectroscopy and Low-Energy Electron Diffraction

Benjamin Young

James Warner
University of Rhode Island

David R. Heskett
University of Rhode Island, dheskett@uri.edu

Follow this and additional works at: https://digitalcommons.uri.edu/phys_facpubs

Citation/Publisher Attribution

Young, B., Warner, J., & Heskett, D. (2015). Ion bombardment of Ni(110) studied with inverse photoemission spectroscopy and low-energy electron diffraction. *Surface Science*, 644, 64-68. doi: 10.1016/j.susc.2015.09.020
Available at: <https://doi.org/10.1016/j.susc.2015.09.020>

This Article is brought to you by the University of Rhode Island. It has been accepted for inclusion in Physics Faculty Publications by an authorized administrator of DigitalCommons@URI. For more information, please contact digitalcommons-group@uri.edu. For permission to reuse copyrighted content, contact the author directly.

Ion Bombardment of Ni(110) Studied with Inverse Photoemission Spectroscopy and Low-Energy Electron Diffraction

The University of Rhode Island Faculty have made this article openly available.
Please let us know how Open Access to this research benefits you.

This is a pre-publication author manuscript of the final, published article.

Terms of Use

This article is made available under the terms and conditions applicable towards Open Access Policy Articles, as set forth in our [Terms of Use](#).

Title: Ion bombardment of Ni(110) studied with inverse photoemission spectroscopy and low energy electron diffraction.

Authors: Benjamin Young^a, James Warner^b, and David Heskett^b

a) Physical Sciences Department

Rhode Island College

600 Mount Pleasant Ave.

Providence, RI 02908, USA

b) Department of Physics

University of Rhode Island

East Hall, 2 Lippitt Rd.

Kingston, RI 02881, USA

Corresponding Author: Dr. Benjamin Young
Physical Sciences Department
Rhode Island College
600 Mount Pleasant Avenue
Providence RI 02908
Phone: 1-401-456-9644
Email: byoung@ric.edu

ABSTRACT

Inverse Photoemission Spectroscopy (IPES) performed on clean Ni(110) reveals an unoccupied electronic surface state with energy ~ 2.5 eV above the Fermi level for emission near the $\bar{\Gamma}$ point of the Surface Brillouin Zone. Ion bombardment of the sample creates defects that reduce the intensity of the peak in IPES spectra. Sharp, intense diffraction spots in Low Energy Electron Diffraction (LEED) patterns taken of the clean surface become dimmer after bombardment. Results of these measurements are compared to Monte Carlo simulations of the sputtering process to ascertain the approximate size of clean patches on the sample necessary to sustain the IPES and LEED features. At 170 K, the IPES surface state peak appears closely associated with the population of surface atomic sites contained in clean circular patches of about 50 atoms. The LEED patterns persist to greater degrees of sputtering and are associated with smaller clean patches. Both measurements performed at 300 K indicate significant self-annealing of the sputtering damage.

Keywords: Inverse Photoemission; Low Energy Electron Diffraction; surface state; ion bombardment; Ni(110)

1. INTRODUCTION

Surface electronic states on metals have been of interest since their observation by Gartland and Slagsvold [1] almost 40 years ago due to their roles in determining electronic and chemical properties of the surface and how they differ from bulk properties [2] [3] [4] [5] [6]. Also of interest, for fundamental understanding as well as for development of technologies on controlled systems which more closely approximate real-life surfaces, investigations into defects and adsorbed species at surfaces have been studied extensively [7] [8] [9] [10] [11] [12] [13] [14].

Ion bombardment, or sputtering, in itself is a topic of considerable importance. In addition to being the first step in many surface characterization techniques, sputtering can induce nanopatterning of surfaces and is a powerful tool for creating novel materials [13] [14] [15] [16] [17] [18]. Additionally, low energy sputtering may be considered as an inverted layer-by-layer growth (see [15] and references therein).

Morgenstern and coworkers [19] showed surface state depopulation through the disappearance of its characteristic signal in a Scanning Tunneling Microscopy (STM) /Spectroscopy (STS) study of Ag(111) for terraces less than 3.2 nm wide. Pons *et al.* [20] studied the effect of surface state confinement to monatomic step wells on the surface of Ni(111). In that work, the authors characterized differences in STM data due to the surface state expressed in triangular patches created by indenting the surface with the triangular STM tip (12.5 nm on a side). More recently, Ruggiero *et al.* [21] used STM to discover that Cu₂N islands grown on Cu(100) support two surface states for large islands. One state disappeared on islands of less than ~50 atoms and the other persisted down to islands of 12 atoms.

While the size of nanostructures clearly plays a role in the intensity of surface states, temperature is also a factor. In Reflection Anisotropy Spectroscopy (RAS) investigations of clean Cu(110) under low energy noble gas ion bombardment, Martin *et al.* [22] witnessed significantly reduced intensity of the signal due to the ~2 eV surface state at the \bar{Y} point for increasing sample temperatures, but Bremer *et al.* [18] observed no changes in its intensity for sputtering at room temperature. Heskett *et al.* [12] reported, through Inverse Photoemission Spectroscopy (IPES) measurements, that although no change in the surface state intensity was observed for sputtering by 1 keV Ne⁺ at room temperature, it decreased monotonically for similar sputtering at 170 K and suggested a room temperature self-annealing effect.

Furthermore, through simulations of the sputtering process, they predicted that the existence of a well-defined surface state signal in the IPES spectra would require unsputtered square surface patches of about 150 atoms.

RAS experiments can simultaneously observe occupied and unoccupied surface states by measuring transitions between them, and this feature has prompted other explanations for quenching of the unoccupied surface state. Sun *et al.* have observed in multiple studies that the RAS signal indicating transitions between occupied and unoccupied surface states on Cu(110) was strongly attenuated by adsorbates and ascribed this to isotropic scattering-induced depolarization of the occupied state [23] [24] [25]. Martin and coworkers [26] observed a similar reduction in the RAS signal on Ni(110) after adsorption of CO and Na, and noted that the signal was sensitive to the specific sample cleaning procedures before treatment with adsorbates. Furthermore, they identified a broader RAS signal for Ni(110) than was seen in earlier work on Cu(110). Recently, Isted, *et al.* [27] investigated Cu(110) under ion bombardment at normal incidence with RAS, STM and a version of the scattering model developed by Poelsema and Comsa [28]. In that study, the authors find close agreement between their integrated RAS signal intensity at various sputtering doses and the simulated fraction of surface cells not contained in circular patches of about 19 unit cells surrounding defects. This is supported by other studies [29] [30] on the same system with adsorbates and a variety of defects where cells not within ~20 unit cell patches were proposed to support the measurement signal.

In this study we present Low Energy Electron Diffraction (LEED) and Inverse Photoemission investigations carried out at room temperature and 170K on ion-bombarded Ni(110) to further elucidate the process of sputtering at low doses and to understand how sputtering modifies structural and electronic properties of the clean surface. We also compare

these results to Monte Carlo simulations of a sputtered crystal to estimate the size of circular, unsputtered patches of the sample surface associated with the LEED and IPES features.

2. EXPERIMENTAL

All experiments were conducted in an ultra-high vacuum chamber with a base pressure $\sim 7 \times 10^{-11}$ Torr. The chamber is equipped with a home-built angle-resolved inverse photoemission spectrometer and Physical Electronics' Low-Energy Electron Diffraction (LEED) system.

The clean Ni(110) surface was prepared by sputtering incident at 70° relative to the sample normal with 500 eV Ar⁺ ions for 30 min. at an Ar pressure of 5×10^{-5} Torr and an emission current of 20 mA, followed by annealing to 750 K for 5 min. The sample holder was constructed from tantalum foil folded around tungsten wires that are coupled to copper posts fed through a dewar which could be filled with liquid nitrogen for cooling. Sample heating was accomplished by passing a high current through the wires that suspend the sample holder and was monitored by a type-K thermocouple spot-welded to the sample holder.

Ion bombardment of the sample for IPES and LEED measurements was performed by back-filling the chamber with high-purity argon to various pressures in the 10^{-7} or 10^{-6} Torr range, followed by sputtering with 500 eV ions at 70° off-normal incidence and 20 mA emission current. For sputtering at 300K and 170K, the bombardment-induced ion current measured between the sample and ground was 0.23 and $0.035 \mu\text{A cm}^{-2}$, respectively. The ion current dropped by less than 10% in all cases during sputtering and was recorded for use in the sputtering simulations.

2.1. LEED measurements

LEED measurements were performed immediately following each sputtering event, initiated as soon as the sputter gas had been evacuated and the chamber pressure recovered to below 2×10^{-10} Torr. For all measurements in this study, a 120 eV beam energy was used with an emission current of 1 mA, and the phosphor screen voltage was fixed at 5 keV. LEED images were acquired with a home-built CCD camera apparatus affixed to the viewport directly opposite the LEED screen.

Analysis software written in-house was used to analyze the LEED images using a procedure similar to Roučka *et al.*[31] and develop spot intensity profiles. Taking rough locations of the diffraction spots in the clean sample LEED pattern image as input from the user, the software is capable of correcting the spot center pixel values and tracking the slight variations of the centers through the whole progression of images. Once the centers are located, the software calculates data pairs of the average intensity value in each set of nearest neighbor pixels with the radius of the nearest neighbor set. The intensity of a given spot is then computed as the midpoint Riemann sum, above the background level, of the average pixel intensity vs. radius from the center pixel.

2.2. IPES measurements

Immediately following collection of the LEED images, Inverse Photoemission Spectroscopy (IPES) measurements were performed. The IPES instrument is operated in isochromat mode and is comprised of an electron gun of the Erdman-Zipf design [32] to provide electrons over a range of incident energies and a Geiger-Müller Tube to detect photons emitted from the crystal. The detector is filled with helium to 18 Torr (uncorrected pressure read by an N₂-calibrated Convectron gauge), before opening a valve to iodine crystals that are allowed to equilibrate. The entrance window of the detector is a 2.5 mm-thick SrF₂ disc with a diameter of 1". This

arrangement permits detection of photons with 9.5 eV with a bandpass of approximately 0.5 eV as the difference between the photoionization threshold of iodine and the energy cutoff for transmission through the end window [33].

The detector signal was conditioned by a fast-pulse counting circuit, delay line amplifier, and single channel analyzer before being recorded as count rate vs. the energy of electrons incident on the sample from the electron gun. For all spectra taken in this study, the end window of the detector was positioned by a linear manipulator to within 2 cm of the sample surface at 45° relative to the sample normal. The electron gun was aimed 45° off the sample normal direction, which corresponds to the \bar{Y} point of the Ni(110) Surface Brillouin Zone. The electron energies were scanned in steps of 100 meV and held for 250 ms before proceeding to the next energy step. The spectra collected for this study are sums of 50 scans, normalized to the average current developed on the sample at each energy step. IPES spectra of the clean sample showed no changes in feature intensities or locations over a period of a few hours.

2.3. Simulations

A clean 1000 x 1000 atom surface was modeled as an array of zeroes and array elements corresponding to Monte Carlo selected ion impact sites were incremented by one to simulate the sputtering process. To determine the number of ion collisions, we obtained an analytic expression for the ion flux from fits to the sample current data collected during sputtering, an estimation of the ratio of nickel sample area to the total current collection area by image analysis, and the area of the surface unit cell. From this we obtained an average number of collisions per surface atom during an event by integrating over the time range of the event. We assumed each collision with the surface removed, on average, two atoms. This is supported by the conclusions

of Vasylyev and coworkers in their study of low-energy Ar ion bombardment on low index nickel surfaces [34], where it was suggested that low-dose sputtering on this system likely produces vacancy point defects and adatoms with mean damage area per ion collision of about 5 unit cells. We note, however, that other authors have reported various higher estimates for the yield and damaged area per ion impact [27] [34] [35].

For each collision in the simulation, 1-3 atoms were removed from the simulated crystal with equal probability. If one atom was chosen, only the primary atom was removed. If two or three atoms were removed, atoms adjacent to the primary location were also removed with probability based on the geometry of the Ni(110) surface unit cell. The simulated crystal was analyzed to determine the number of atomic sites in the crystal contained in unsputtered patches of radius r , where r was varied. The analysis was run over each subsequent sputtering increment to develop curves corresponding to each value of r to define $f(\theta)^r$, the relative population of surface atoms in patches of unsputtered atomic radius r , as a function of θ (equivalent monolayers removed). We also calculated θ values for the IPES and LEED experiments.

3. RESULTS

3.1. LEED measurements

Images taken of characteristic LEED patterns during a progression of sputtering, up to a cumulative bombardment time of 26 minutes, by 500 eV Ar⁺ ions at 170K were analyzed to produce the plot in Figure 3. The integrated intensity of the (1,-1) diffraction spot, normalized to the intensity of the clean image is displayed relative to the sputtering dose as equivalent monolayers removed.

3.2 IPES measurements

Characteristic spectra from the IPES measurements are displayed in Figure 1. Data were collected when the sample was sputtered by 500 eV ions at an argon pressure of 2×10^{-7} Torr while cooled with liquid nitrogen in (a) and for room temperature sputtering with argon $p = 1 \times 10^{-6}$ in (b). The count rate is plotted on the y-axis as intensity and the scale of the electron kinetic energy on the x-axis has been shifted to align 0 eV with the half-rise location of the Fermi edge energy, E_F . The traces correspond to IPES spectra taken after the cleaning procedure and then after each subsequent sputtering event, and are offset vertically for display purposes. The intensity of the surface state feature decreases monotonically with cumulative sputtering damage and appears to (nearly) reach a steady state by 0.05 ML removal of the surface. The total intensity of the surface state feature was calculated relative to a linear background for each spectrum. We observed no broadening of the surface state peak under ion bombardment, which we also noted to be the case within the resolution limit of our analyzer in an earlier study on sputtering of Cu(110) [12].

3.3. Simulations

Selected results of the sputtering model on small areas of the larger simulated crystal are shown in Figure 2. Each panel is labeled with the θ value (equivalent monolayer removed) appropriate to the larger simulated crystal. Sites where sputtering has removed a surface atom are shown as greyscale disturbances on the otherwise white background representing areas untouched by the bombardment process. Black represents the site(s) in each simulated crystal where the largest number of atoms has been removed from a single site (usually 2 or less). Because the second layer atoms of a face-centered cubic (110) surface are not directly beneath

those of the first layer, the analysis considers only the top layer. Curves corresponding to the relative population of surface atoms in clean patches of atomic radius r , as a function of θ , are displayed in Figure 3. One trace is displayed per integer value of r . For all values of r the intensity function decreases with apparent exponential behavior in θ and the decrease is faster for successively higher values of r . This behavior is different from that observed in [12], where square clean patches were used as the search criteria, indicating there is some dependence of the model on the shape of the search criterion at low-doses. While the intensity of the simulated curves also decreased monotonically there, the shape resembled a half-Gaussian. Our present simulation yields curves similar to the ones reported in [12] if square patches are used to search the simulated crystal. It is also worth noting that the simulation in [12] assumed the ion flux to be constant during sputtering and did not account for the portion of the measured ion current due to collisions with the sample mounting. We have accounted for these factors in the present model and believe it better represents the observed trends.

4. DISCUSSION

A summary of the results from techniques applied in this study is displayed in Figure 3 for the experiment conducted at 170 K. The IPES surface state peak intensity appears to decrease along with the prevalence of untouched circular patches of radius 4 atoms. From this we estimate that the minimum circular patch size necessary to sustain the surface state in these measurements is approximately 50 atoms. This agrees very well with the work of Ruggiero *et al.*, who reported that a surface state observed for nanoscale Cu_2N islands on Cu(100) disappears on islands with fewer than ~ 50 atoms at 5.3 K [21]. Investigations of surface states on terraces and in confinement regions have produced comparable or higher estimates for necessary areas

[19] [20]. It should be noted that these experiments were conducted at lower temperatures than we are able to achieve in our current setup.

In our previous study [12], we found no obvious change in the intensity of the IPES surface state peak observed on Cu(110) for sputtering at room temperature, but performed at 170 K, the sputtering process did reduce its intensity to near zero. For the present work, we were able to decrease the intensity of the Ni(110) surface state by room temperature sputtering, as displayed in Figure 1b indicating that thermal self-annealing at room temperature is less effective for Ni(110) than was true for Cu(110), consistent with the higher Debye temperature for Ni versus Cu. Analysis of the intensity decrease relative to the amount of sputtering damage using the yield estimates described above indicate that the surface state feature in the IPES spectra requires approximately 10 times the sputtering dose to achieve comparable intensity reduction at room temperature as when the experiment is performed at 170 K. The model does not account for the self-annealing effect, so we expect it to underestimate the necessary patch size for experiments performed at temperatures where self-annealing occurs faster than data collection can be accomplished. This is obviously the case for the room temperature measurement, though it is unclear whether 170 K is a sufficiently low temperature to eliminate the effect.

Given the relatively low sputtering dose observed to quench the IPES signal, we believe this simple model gives reliable results. The larger effective defect radius for a single ion impact revealed in other studies [27] [34] [35] would cause the simulated curves to decrease in intensity for lower sputter doses, and would more quickly approach zero intensity, but these effects do not change our results for the range of sputtering and necessary patch size presented. To verify this, the simulation was also performed assuming 0-2 atom removal per ion collision, effectively decreasing the mean ion damage area in the simulation with little change to the results displayed.

Similarly subtle results follow for small increases to the mean damage area. Thus, we believe the estimate that the IPES surface state feature requires clean patches of ~50 atoms to represent a reasonable result.

The LEED spots appear to more quickly approach an asymptotic intensity level (~40% relative to clean) than the IPES feature, and when compared to the Monte Carlo results, behave most similarly to curves for simulated clean patches of atomic radius 2-3 at 170 K. It is not surprising that the LEED spots' intensity is tied to smaller clean patches than the IPES surface state intensity. The LEED measurement takes information from deeper than IPES [34] and the simulation concerns only the top layer of the surface. Thus, it is to be expected that the LEED features are less sensitive to the order of the topmost layer, which our analysis indicates.

An important question remains, however, as to the nature of the quenching observed for the surface state in the IPES spectra. Our analysis supports the conclusion that the intensity of the surface state is tied to the existence of clean patches of about 50 atoms. A competing, though not necessarily conflicting view is described chiefly by the RAS studies dealing with adsorbates and defects on Cu(110) [22] [23] [24] [25] [26] [27]. The reduced RAS signal these authors observe may be due to destruction of the unoccupied state as we suggest. If vacancy defects essentially remove the ability of the surface to sustain the unoccupied state, any measured intensity of transitions between it and occupied states would be reduced. It is also possible, as they argue, that isotropic scattering from defects (adsorbates) may be the mechanism responsible for quenching the RAS signal as an occupied state effect. Because neither RAS nor IPES can independently measure both the unoccupied and the occupied state intensity simultaneously, it is not clear whether the decreased RAS and IPES signals may be ascribed to either proposed mechanism or a combination of the two.

From the sample drain current during sputtering, we estimate an ion flux of 6.5×10^{-5} ions/unit cell/s for the experiment performed at 170 K. This is roughly 20 times less than what was reported by Isted et al. [27] for 145K sputtering of Cu(110). In that study, the authors showed approximately 90% reduction of the clean sample RAS signal for 12s of sputtering at the higher ion flux. The sputtering time necessary to reduce our IPES signal on clean Ni(110) by 90% is greater than this by a factor of about 75, in excess of what might be expected for the difference in ion flux alone. We believe this comparison supports the conclusion that the RAS signal may be quenched more quickly than the IPES signal for comparable sputtering amounts.

5. CONCLUSIONS

Argon ion bombardment of Ni(110) has been investigated at room temperature and at 170 K by IPES, LEED, and computer simulations. Bombardment-associated effects on the intensity of the unoccupied surface electronic state near the $\bar{\Gamma}$ point of the Surface Brillouin Zone in IPES spectra, as well as on the intensity profiles of diffraction spots in LEED patterns have been obtained. Monotonic reduction of the intensities of the features in both IPES and LEED results are compared to the simulations of sputtering to determine 50 atoms as the size of clean surface patches necessary to sustain the surface state in IPES spectra. Both the LEED and IPES measurements exhibit thermal self-annealing effects at room temperature that are reduced at 170 K.

6. ACKNOWLEDGEMENTS

This work was partially supported by grants from the EGRA program at the University of Rhode Island and from the Rhode Island College Faculty Research Fund (grant 80000429).

7. REFERENCES

- [1] P. Gartland and B. Slagsvold, "Transitions conserving parallel momentum in photoemission from the (111) face of copper," *Phys. Rev. B*, vol. 21, p. 4047, 1975.
- [2] A. Goldmann, M. Donath, W. Altmann and V. Dose, "Momentum-resolved inverse photoemission study of nickel surfaces," *Phys. Rev. B*, vol. 32, no. 2, pp. 837-850, 1985.
- [3] A. Goldmann, V. Dose and G. Borstel, "Empty electronic states at the (100), (110), and (111) surfaces of nickel, copper, and silver," *Phys. Rev. B*, vol. 32, no. 4, pp. 1971-1980, 1985.
- [4] O. Zeybek, A. Davarpanah and S. Barrett, "Electronic surface states of Cu(110) surface," *Surf. Sci.*, vol. 600, pp. 5176-5181, 2006.
- [5] N. Biswas, J. Gurganus and V. Misra, "Work function tuning of nickel silicide by co-sputtering nickel and silicon," *Appl. Phys. Lett.*, vol. 87, p. 171908, 2005.
- [6] J. Li, W. Schneider, R. Berndt, O. Bryant and S. Crampin, "Surface-State Lifetime Measured by Scanning Tunneling Microscopy," *Phys. Rev. Lett.*, vol. 81, no. 20, pp. 4464-4467, 1998.
- [7] T. Allmers, M. Donath, J. Braun, J. Minar and H. Ebert, "d- and sp- like surface states on fcc Co(001) with distinct sensitivity to surface roughness," *Phys. Rev. B*, vol. 84, p. 245426, 2011.
- [8] E. Boschung, T. Pillo, J. Hayoz, L. Patthey, P. Aebi and L. Schlapbach, "Hydrogen-induced changes in the surface states/resonances of Ni(100)," *J. Electron Spectrosc. Relat. Phenom.*, Vols. 101-103, pp. 349-353, 1999.
- [9] S. Yu, B. Bahrim, B. Makarenko and J. Rabalais, "Local effect of Na adsorption on Cu(111)," *Surf. Sci.*, vol. 606, pp. 1700-1704, 2012.
- [10] D. Tang and D. Heskett, "Unoccupied electronic structure of Na/Ni(111)," *Phys. Rev. B*, vol. 47, no. 16, pp. 695-699, 1993.
- [11] C. Su, D. Tang and D. Heskett, "Two-dimensional unoccupied electronic band structure of clean Cu(110) and (1x2) Na/Cu(110)," *Surf. Sci.*, vol. 310, pp. 45-51, 1994.
- [12] D. Heskett, D. DePietro, G. Sabatino and M. Tamaro, "Ion bombardment-induced changes in the electronic structure of Cu(110) investigated with inverse photoemission and computer simulations," *Surf. Sci.*, vol. 513, pp. 405-411, 2002.
- [13] O. Rodríguez de la Fuente, M. González-Barrio, V. Navarro, B. Pabón, I. Palacio and A. Mascareque, "Surface defects and their influence on surface properties," *J. Phys.: Condens. Matter*, vol. 25, no.

48, p. 484008, 2013.

- [14] J. Bellina and H. Farnsworth, "Ion Bombardment Induced Surface Damage in Tungsten and Molybdenum Single Crystals," *J. Vac. Sci. Technol.*, vol. 9, no. 2, pp. 616-619, 1972.
- [15] W. Chan and E. Chason, "Making waves: Kinetic processes controlling surface evolution during low energy ion sputtering," *J. Appl. Phys.*, vol. 101, p. 121301, 2007.
- [16] X. Ou, R. Kögler, X. Wei, A. Mücklich, X. Wang, W. Skorupa and S. Facsko, "Fabrication of horizontal silicon nanowire arrays on insulator by ion irradiation," *AIP Advances*, vol. 1, p. 042174, 2011.
- [17] A. Biermanns, A. Hanisch, J. Grenzer, T. Metzger and U. Pietsch, "Tuning the shape and damage in ion-beam induced ripples on silicon," *Phys. Status Solidi A*, vol. 208, no. 11, pp. 2608-2611, 2011.
- [18] J. Bremer, J. Hansen and O. Hunderi, "The effect of sputtering-induced disorder on the surface dielectric tensor of Cu(110)," *Surf. Sci.*, vol. 436, pp. L735-L739, 1999.
- [19] K. Morgenstern, K. Braun and K. Rieder, "Surface-State Depopulation on Small Ag(111) Terraces," *Phys. Rev. Lett.*, vol. 89, no. 22, p. 226801, 2002.
- [20] S. Pons, P. Mallet, L. Magaud and J. Veuillen, "Investigation of the Ni(111) Shockley-like surface state using confinement to artificial nanostructures," *Europhys. Lett.*, vol. 61, no. 3, pp. 375-381, 2003.
- [21] C. Ruggiero, M. Badal, T. Choi, D. Gohlke, D. Stroud and J. Gupta, "Emergence of surface states in nanoscale Cu₂N islands," *Phys. Rev. B*, vol. 83, p. 245430, 2011.
- [22] D. Martin, A. Maunder and P. Weightman, "Thermal Behaviour of the Cu(110) surface studied by reflection anisotropy spectroscopy and scanning tunneling microscopy," *Phys. Rev. B.*, vol. 63, p. 155403, 2001.
- [23] L. D. Sun, M. Hohage, P. Zeppenfeld, R. E. Balderas-Navarro and K. Hingerl, "Enhanced Optical Sensitivity to Adsorption due to Depolarization of Anisotropic Surface States," *Phys. Rev. Lett.*, vol. 90, no. 10, p. 106104, 2003.
- [24] L. D. Sun, M. Hohage, R. Denk and P. Zeppenfeld, "Oxygen adsorption on Cu(110) at low temperature," *Phys. Rev. B*, vol. 76, p. 245412, 2007.
- [25] L. D. Sun, R. Denk, M. Hohage and P. Zeppenfeld, "Scattering of surface electrons from CuO stripes on Cu(110)," *Surf. Sci.*, vol. 602, p. L1, 2007.
- [26] D. S. Martin, S. D. Barrett and P. Weightman, "Reflection anisotropy spectroscopy of clean and adsorbate-covered Ni(110) surfaces," *J. Phys.: Condens. Matter*, vol. 13, pp. 9847-9855, 2001.

- [27] G. E. Isted, P. D. Lane, R. J. Cole, M. Caffio and R. Schaub, "Estimating the range of influence of point defects on Cu(110) surface states," *Phys. Rev. B*, vol. 83, p. 155403, 2011.
- [28] B. Poelsema and G. Gomsa, *Scattering of Thermal Energy Atoms*, Springer Tracts in Modern Physics, Berlin: Springer, 1989.
- [29] P. Lane, G. Isted and R. Cole, "Effect of surface defects and adsorbates on the optical anisotropy of Cu(110)," *Phys. Rev. B*, vol. 82, p. 075416, 2010.
- [30] P. D. Lane, D. S. Martin, D. Hesp, G. E. Isted and R. J. Cole, "Effects of steps and ordered defects on Cu(110) surface states," *Phys. Rev. B*, vol. 87, p. 245405, 2013.
- [31] R. Roucka, J. Jiruse and T. Sikola, "Spot intensity processing in LEED images," *Vacuum*, vol. 65, pp. 121-126, 2002.
- [32] P. Erdman and E. Zipf, "Low Voltage, High Current Electron Gun," *Rev. Sci. Instrum.*, vol. 53, pp. 225-227, 1982.
- [33] M. Budke, V. Renken, H. Liebl, G. Rangelov and M. Donath, "Inverse photoemission with energy resolution better than 200 meV," *Rev. Sci. Instrum.*, vol. 78, p. 083903, 2007.
- [34] M. Vasylyev, A. Blaschuk, N. Mashovets and N. Vilkova, "LEED study of Ni(100) and (111) surface damage caused by Ar⁺ ion bombardment with low energy and small doses," *Vacuum*, vol. 57, pp. 71-80, 2000.
- [35] T. Michely and G. Comsa, "Temperature dependence of the sputtering morphology of Pt(111)," *Surf. Sci.*, vol. 256, no. 3, pp. 217-226, 1991.

8. FIGURES

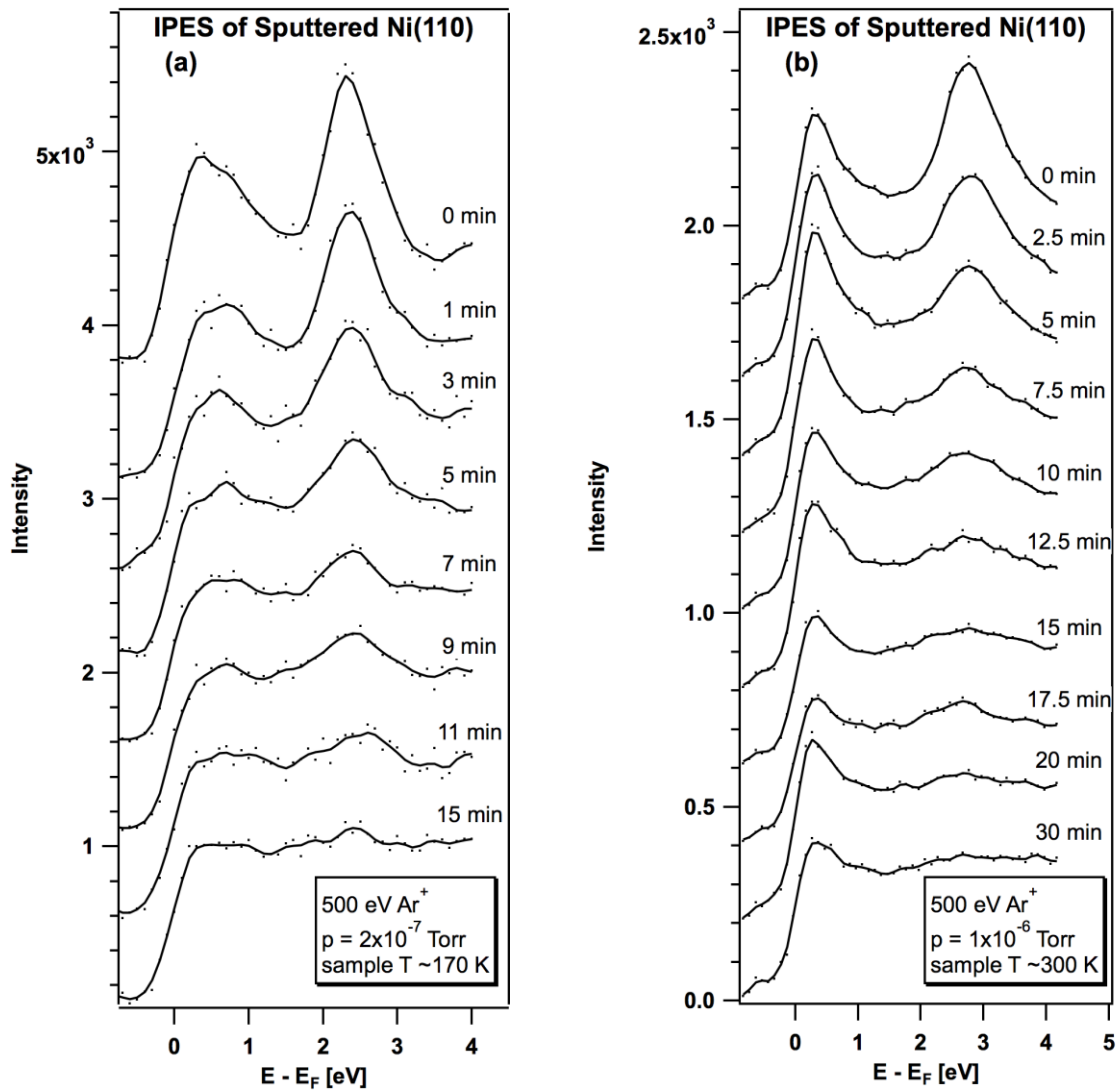


FIG. 1. Inverse Photoemission spectra of the Ni(110) surface sputtered by 500 eV in an Ar atmosphere for various sputtering times at 70° degree incidence from the sample normal. The spectra were recorded for a geometry corresponding to emission from the \bar{Y} point. The sample was held at; (a) $T \sim 170 \text{ K}$ and sputtering performed at $p = 2 \times 10^{-7}$ or; (b) $T \sim 300 \text{ K}$ and sputtering performed at $p = 1 \times 10^{-6} \text{ Torr}$.

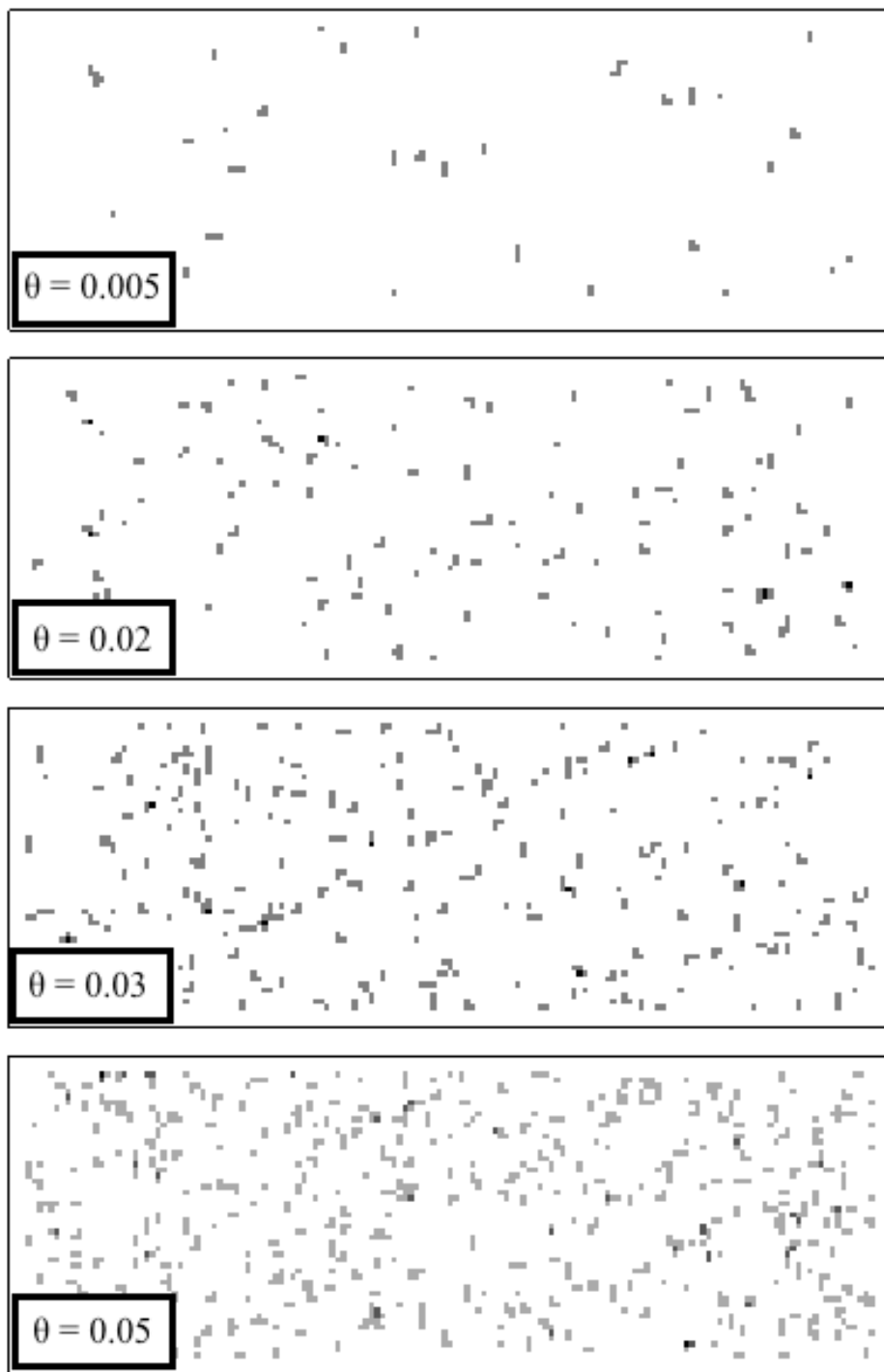


FIG. 2. Simulated sputtered crystal representations for $\theta = \{0.005, 0.02, 0.03, 0.05\}$ ML removed. White areas represent patches of unsputtered atoms and sites where atoms have been removed are darker.

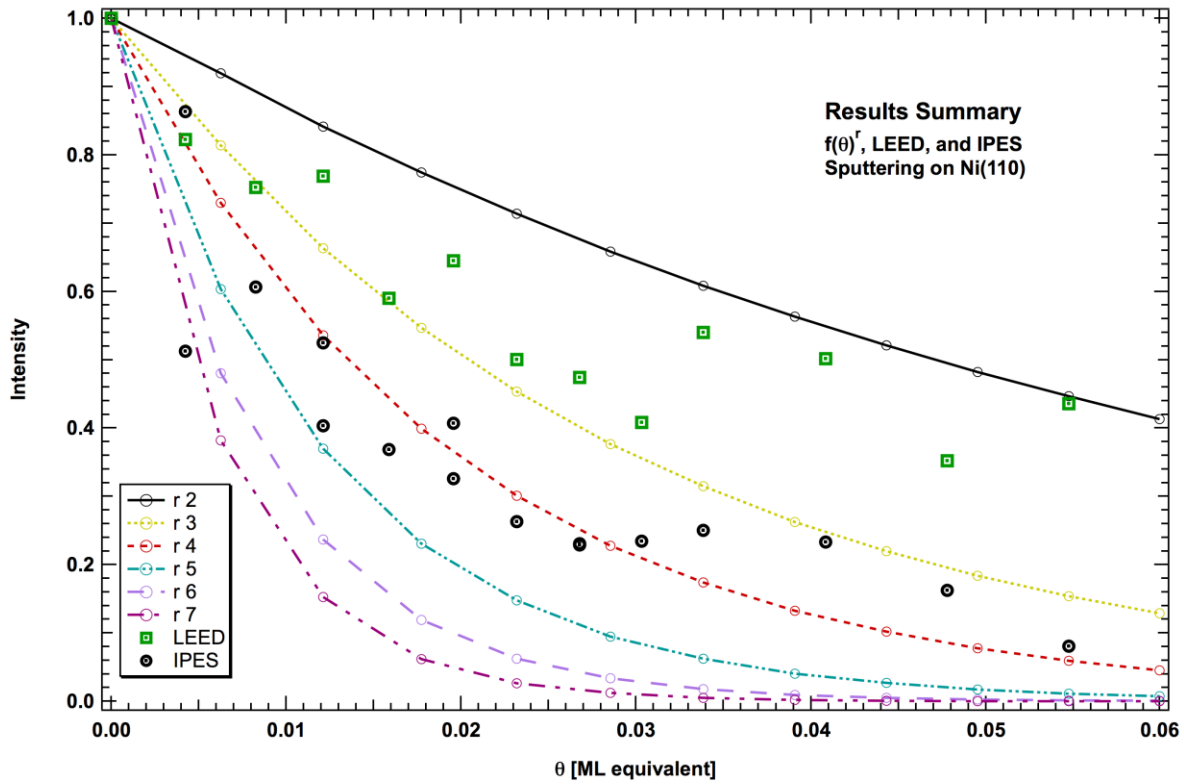


FIG. 3. LEED (green squares) and IPES (black circles) overlaid on the simulation results. Simulation results corresponding to clean patch radii of N atoms are labeled “ $r N$.” The LEED and IPES intensities have been normalized to those of the clean sample.